Quantum unified theory applied to Lybeta, Lygamma and Lydelta electronic Stark broadening

Amaury de Kertanguy, Nicole Feautrier, O. Motapon

A&A 432, 1131–1135 (2005)
DOI: 10.1051/0004-6361:20042167

Astronomy & Astrophysics

Quantum unified theory applied to Lyβ, Lyγ and Lyδ electronic Stark broadening

A. de Kertanguy, N. Feautrier, and O. Motapon⋆

LERMA and UMR 8112 du CNRS, Observatoire de Paris, 92195 Meudon Cedex, France
e-mail: amaury.dekertanguy@obspm.fr

Received 13 October 2004 / Accepted 17 November 2004

Abstract. New quantum calculations for the Lyβ, Lyγ, Lyδ profiles perturbed by electron collisions are obtained from the unified one-perturber theory in the exact resonance approximation (Tran-Minh et al. 1975, J. Phys. B: Atom. Molec. Phys., 8, 1810; Feautrier et al. 1976, J. Phys. B: Atom. Molec. Phys., 9, 1871). This accounts for the-long range dipole interaction. The profiles are obtained by summing the partial contributions of each total angular momentum L^{T}. It appears that there is a threshold L_{min} below which some eigenchannels become complex and are not well described by the exact resonance method. To overcome this problem, the contribution of the first angular momenta is estimated by taking into account the real eigenvalues and by neglecting the complex ones. Estimation of the error due to this systematic underestimation of the profile is given. Density effects due to the Debye screening are found in the near wings.

Key words. atomic data – line: profiles – stars: atmospheres – atomic processes

1. Introduction

We present a quantum treatment of the wing profiles of Lyβ, Lyγ, Lyδ lines perturbed by electron collisions. Simultaneous strong collisions are improbable at the typical densities of stellar atmospheres, therefore the one-perturber approach is valid. An exact quantum expression for the hydrogen line profiles was given by Van Regemorter (1969) and Tran-Minh & Van Regemorter (1972). Detailed calculations have been performed for the Lyman α (Feautrier et al. 1976; Feautrier & Tran-Minh 1977; Tran-Minh et al. 1980) and Balmer β (de Kertanguy et al. 1979) line profiles.

The semiclassical electronic profile calculations (assuming straight classical paths for the perturbers) provide a good description of the line center and of the near wing but fail in the far wings where the broadening mechanism is dominated by close collisions. In those regions of the profile, our theoretical description is based upon the so-called *one electron theory* which considerably simplifies the statistical problem of combining the effects of the different perturbers and allows an accurate quantum treatment in regard with the strongly perturbing nature of the interaction (Baranger 1958).

The profile is given as a sum over the total angular momenta L^{T} of partial intensities expressed in terms of overlap integrals of the perturber wave-functions. The exact resonance approximation, described by Seaton (1961), makes exact allowance for the long-range dipole ineraction. In this approach, the electrostatic potential with the centrifugal energy can be diagonalized leading to $\mu_{\mathrm{m}}(\mu_{\mathrm{m}}+1)/r^2$ eigenvalues and $J_{\mu_{\mathrm{m}}+1/2}(Kr)$ eigenfunctions. The μ_{m} values are real for $L^{\mathrm{T}} > L_{\mathrm{Min}}$ but some of them are complex for $L^{\mathrm{T}} < L_{\mathrm{Min}}$. L_{min} depends on the principal quantum numbers of the initial and final levels of the considered lines. Complex values of μ_{m} corresponding to short-range interactions are not well described by the exact resonance approach. For these low angular momenta $L^{\mathrm{T}} < L_{\mathrm{Min}}$, we take into account all real μ_{m} values and neglect the complex ones so that this procedure gives a lower bound of the exact profile. We compare the results with the empirical estimation previously used in Motapon (1998).

The sum of partial intensities is limited at $L^{\mathrm{T}}_{\mathrm{Max}} \approx K\rho_{\mathrm{D}}$ where ρ_{D} is the Debye radius and K is the relative motion wave number defined by $\hbar^2K^2/2m = E$ where E is the kinetic energy of the collision. Different temperatures and densities yield different cutoffs inducing profile variations with temperatures and densities.

In the next section, we give the general expression of the profile; we describe the exact resonance method in Sect. 3. The new results for Lyβ, Lyγ and Lyδ lines are given in Sect. 4.

2. The quantum formula

We are interested in the i→f transition from the initial upper state i to the final state f ($n_{\mathrm{f}} = 1$ for the Lyman series). We define a channel Γ by a set of quantum numbers $\Gamma \equiv nLSl1/2L^{\mathrm{T}}S^{\mathrm{T}}$ where $l1/2$ defines the state of the scattered electron and nLS the state of the atom, L^{T} and S^{T} are respectively the total angular momentum and the total spin of the H + e system.

⋆ *Present address:* Faculté des Sciences, Université de Douala, BP 8580, Douala, Cameroun.

In the one perturber approximation, valid in the wings of a line, the quantum line profile $I(\Delta\omega)$ is given by (Tran-Minh et al. 1975):

$$I(\Delta\omega) = N_{\rm e}\frac{|\langle L_{\rm f}S_{\rm f}||d_1||L_{\rm i}S_{\rm i}\rangle|^2}{(2S_{\rm i}+1)(2L_{\rm i}+1)} \times \int_0^\infty \hbar\rho(\epsilon_{\rm i'})f(\epsilon_{\rm i'})\mathrm{d}\epsilon_{\rm i'}\frac{(2\pi)^3}{4K_{\rm i'}K_{\rm f}} \times \sum(2S_{\rm i}^{\rm T}+1)(2L_{\rm i}^{\rm T}+1)\delta_{l_{\rm i}l_{\rm f}} \times \left|\int_0^\infty \mathrm{d}rG^*(\Gamma_{\rm f}|\Gamma_{\rm f}|r)G(\Gamma_{\rm i'}|\Gamma_{\rm i}|r)\right|^2 \quad (1)$$

where $N_{\rm e}$ is the electron density, $\rho(\epsilon_{\rm i'}) = \frac{m\hbar K_{\rm i'}}{(2\pi\hbar)^3}$ is the energy density of the initial state, $\epsilon_{\rm i'}$ is the kinetic energy of the perturber when the atom is in the i′ state, $f(\epsilon_{\rm i'})$ is the kinetic Maxwell energy distribution. $K_{\rm i'}$ and $K_{\rm f}$ are the wave numbers of the initial and final channels respectively. $|\langle L_{\rm f}S_{\rm f}||d_1||L_{\rm i}S_{\rm i}\rangle|$ is the reduced matrix element of the atomic dipole. The sum Σ extends over $l_{\rm i}L_{\rm i}^{\rm T}S_{\rm i}^{\rm T}n_{\rm i}'L_{\rm i}'l_{\rm i}'$, $L_{\rm f}^{\rm T} = l_{\rm f}$ for the Lyman lines.

The frequency ω of the light emitted is expressed in terms of the kinetic energy of the perturber when the atom is in the i or f state with energy $E_{\rm i}$ or $E_{\rm f}$:

$$\hbar\omega = E_{\rm i} + \frac{1}{2}mv_{\rm i}^2 = E_{\rm f} + \frac{1}{2}mv_{\rm f}^2 \quad (2)$$

and the detuning $\Delta\omega$ is defined by:

$$\hbar\Delta\omega = \frac{1}{2}m(v_{\rm i}^2 - v_{\rm f}^2). \quad (3)$$

The radial wave-functions $G(\Gamma_{\rm i'}|\Gamma_{\rm i}|r)$ are defined in terms of the initial and final channels $\Gamma_{\rm i'}$ and $\Gamma_{\rm i}$ for the collision problem of the upper level i. Expanding the total wave function in terms of the set of atomic wave functions (Percival & Seaton 1957), we find for each $L_{\rm i}^{\rm T}$ and $S_{\rm i}^{\rm T}$ a set of coupled equations for the $G(\Gamma_{\rm i'}|\Gamma_{\rm i}|r)$ functions. It is well known that the interaction between the electron and the H atom in the lower state is negligible for Lyman lines. Therefore $G(\Gamma_{\rm f}|\Gamma_{\rm f}|r)$ is the radial part of a plane wave:

$$G(\Gamma_{\rm f}|\Gamma_{\rm f}|r) = -2\mathrm{i}\sqrt{\frac{\pi r}{2}}J_{l_{\rm f}+1/2}(K_{\rm f}r) \quad (4)$$

where $J_{l_{\rm f}+1/2}$ is the cylindrical Bessel function.

The problem is how to calculate the overlap integrals:

$$I(\mathrm{i}'|\mathrm{i}) = \int_0^\infty \mathrm{d}rG^*(\Gamma_{\rm f}|\Gamma_{\rm f)}|r)G(\Gamma_{\rm i'}|\Gamma_{\rm i}|r). \quad (5)$$

3. Radial wave functions and overlap integrals

3.1. The exact resonance method

The $I(\Delta\omega)$ profile can be expressed as a sum over the total angular momentum $L_i^{\rm T}$ of the system (see Eq. (1)). We write:

$$I(\Delta\omega) = \sum_{L_{\rm i}^{\rm T}=0}^{L_{\rm D}} I_{L^{\rm T}} \quad (6)$$

where the cut-off $L_{\rm D}$, corresponding to the Debye radius, takes into account the screening by the other electrons. Leaving apart the problem of the first angular momenta $L_{\rm i}^{\rm T}$ for which special treatments are necessary (Feautrier et al. 1976; Feautrier & Tran-Minh 1977; Motapon 1998), we focus our attention on the larger values of $L_{\rm i}^{\rm T}$. Exchange is not important and the dipolar part of the potential is predominant.

Retaining only asymptotic forms of the dipole potential, the exact resonance method of Seaton (1961) yields the following coupled equations:

$$r^2\left(\frac{\mathrm{d}^2}{\mathrm{d}r^2} + \boldsymbol{K}_{\rm i}{}^2\right)\boldsymbol{G} = \boldsymbol{A}\boldsymbol{G} \quad (7)$$

where $\boldsymbol{A}/r^2$ contains the dipolar potentials $\boldsymbol{V}_{{\rm i}j}$ and centrifugal terms.

Two sets of coupled equations must be solved, according to the total parity $\pi_{\rm i} = (-1)^{l_{\rm i}}$ or $\pi_{\rm i} = (-1)^{l_{\rm i}+1}$. To solve Eq. (7), we diagonalize $\boldsymbol{A}$. We obtain eigenvalues $a_{\rm m}$ and the unitary matrix of eigenvectors $\boldsymbol{X}$. The system is equivalent to:

$$r^2\left(\frac{\mathrm{d}^2}{\mathrm{d}r^2} + \boldsymbol{K}_{\rm i}^2\right)\boldsymbol{\mathcal{G}} = \boldsymbol{a}\boldsymbol{\mathcal{G}} \quad (8)$$

where $\boldsymbol{a}$ is the diagonal matrix whose elements are $a_{\rm m}$. Setting $a_{\rm m} = \mu_{\rm m}(\mu_{\rm m}+1)$ the solutions are:

$$g_{\rm mm}(r) = -\mathrm{i}\sqrt{2\pi r}J_{\mu_{\rm m}+1/2}(K_{\rm i}r)\exp\left(-\mathrm{i}\frac{\mu_{\rm m}\pi}{2}\right). \quad (9)$$

By a unitary transformation we obtain:

$$G(\Gamma_{\rm i'}|\Gamma_{\rm i}|r) = \exp\left(il_{\rm i'}\frac{\pi}{2}\right)(\boldsymbol{X}\boldsymbol{\mathcal{G}}\boldsymbol{X}^{-1})_{\rm i'i}. \quad (10)$$

Analytical solutions for the $\mu_{\rm m}$ are only obtained for the level $n = 2$ (Tran-Minh et al. 1980). For $n > 2$ we must perform the numerical diagonalization of the $\boldsymbol{a}$ matrix; we evaluate the quantity:

$$\mu_{\rm m} = -\frac{1}{2} + \frac{1}{2}\sqrt{1+4a_{\rm m}}. \quad (11)$$

The condition $1 + 4a_{\rm m} = 0$ determines the lower value $L_{\rm min}^{\rm T}$ of the total angular momentum for which all the eigenvalues are real.

Following Tran-Minh et al. (1975), Feautrier et al. (1976), Feautrier & Tran-Minh (1977), Motapon (1998), the overlap integrals are, for $L_i^{\rm T} \geq L_{\rm min}^{\rm T}$, linear combinations of integrals of the form:

$$\mathcal{I}(\mu_{\rm m}, K_{\rm i}, l_{\rm f}, K_{\rm f}) = \int_0^\infty \frac{1}{r}J_{\mu_{\rm m}+1/2}(K_{\rm i}r)J_{l_{\rm f}+1/2}(K_{\rm f}r)\mathrm{d}r. \quad (12)$$

These integrals are known in terms of hypergeometric functions (Gradshteyn & Ryzhik 1965):

$$F\left(\frac{\mu_{\rm m}+l_{\rm f}+1}{2}, \frac{-\mu_{\rm m}+l_{\rm f}}{2}, l_{\rm f}+\frac{3}{2}; \frac{K_{\rm f}^2}{K_{\rm i}^2}\right) \quad \text{for } K_{\rm i} > K_{\rm f}$$

$$F\left(\frac{\mu_{\rm m}+l_{\rm f}+1}{2}, \frac{\mu_{\rm m}-l_{\rm f}}{2}, \mu_{\rm m}+\frac{3}{2}; \frac{K_{\rm i}^2}{K_{\rm f}^2}\right) \quad \text{for } K_{\rm f} > K_{\rm i}.$$

Averaging over the initial energies in Eq. (1) implies integration over $\epsilon_{\rm i'}$ from zero to infinity. However it is necessary to have $\frac{1}{2}mv_{\rm f}^2 \geq 0$, therefore $\epsilon_{\rm i'} \geq \hbar\Delta\omega$. Thus the lower integration limit is $\epsilon_{\rm min} = 0$ for $\Delta\omega < 0$ and $\epsilon_{\rm min} = \hbar\Delta\omega$ for $\Delta\omega > 0$. As a consequence, a full velocity average must be carried out.

Table 1. Number of channels and minimum value of the total angular momentum for each parity in the exact resonance theory.

Level	$\pi_i = (-1)^{l_i}$		$\pi_i = (-1)^{l_i+1}$	
	m	L^T_{min}	m	L^T_{min}
$n = 2$	3	3	1	0
$n = 3$	6	5	3	3
$n = 4$	10	7	6	5
$n = 5$	15	9	10	7

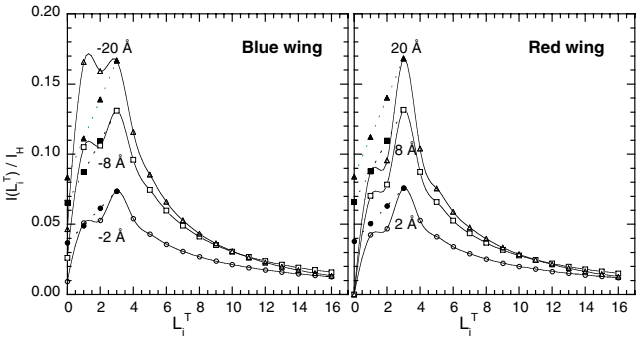

Fig. 1. Contributions of the first angular momenta to the Lyman α profile. Full curve: this work, dotted curve: Motapon (Motapon1988)

3.2. Contribution of the low angular momenta

The number m of channels required for the collisional treatment increases as n^2, this prohibits refinements such as exchange effects and introduction of short range potentials taken into account in the Lyα calculations. However, the exact resonance method fails for low angular momenta as some μ_m values become complex leading to resonances in the cross sections. Table 1 gives the values of L^T_{min} and m for levels $n = 2, 3, 4, 5$ relevant for the Lyα, Lyβ, Lyγ and Lyδ lines and for the two parities of the (H+e) total system.

We give in Appendix A the numerical values of the μ_m calculated for the $n = 3$ level. These numbers were calculated using Mathematica. It appears (see Table A.1) that, for the $(-1)^{l_i}$ parity, only one μ_m value among six is complex for $L^T_i = 3, 4$, two μ_m values are complex for $L^T_i = 1, 2$ and three μ_m for $L^T_i = 0$. For the $(-1)^{l_i+1}$ parity (Table A.2), there is no complex value for $L^T_i = 3, 4$, one is complex for $L^T_i = 1, 2$ and two are complex for $L^T_i = 0$. The same trend exists for higher n-levels. So the number of complex channels is small and limited to the first angular momenta and we have adopted the following procedure in the calculations: we have taken into account all the real μ values in the summation involved in the matrix product (see Eq. (11)) and we have neglected the contribution of the complex μ values. As a consequence, the final result is a lower limit of the exact value since all the contributions are positive (see Eq. (1)).

Figure 1 compares at $T = 12\,200$ K, for three blue and red detunings of the Lyman α line, the contributions (normalized to the Holtsmark intensity) of the first angular momenta obtained in our calculations with the extrapolation procedure used in Motapon (1988).

The results are quite similar in the near wing, but systematic differences occur for large detunings: our results are larger in the blue wing and lower in the red wing, and the differences which are very small for $\Delta\lambda = 2$ increase with $\Delta\lambda$. If we recall that our procedure gives a lower limit of the profile, the extrapolation procedure of Motapon (1998) appears to underestimate the intensity in the blue wing and thus to overestimate the asymmetry between the two wings. In fact the correct result should take into account the short range interactions that are important for these low angular momenta (Feautrier et al. 1976). Hopefully, the contribution of these first angular momenta is almost negligible in the near wing (less than 1%) and increases very slowly when the detuning increases.

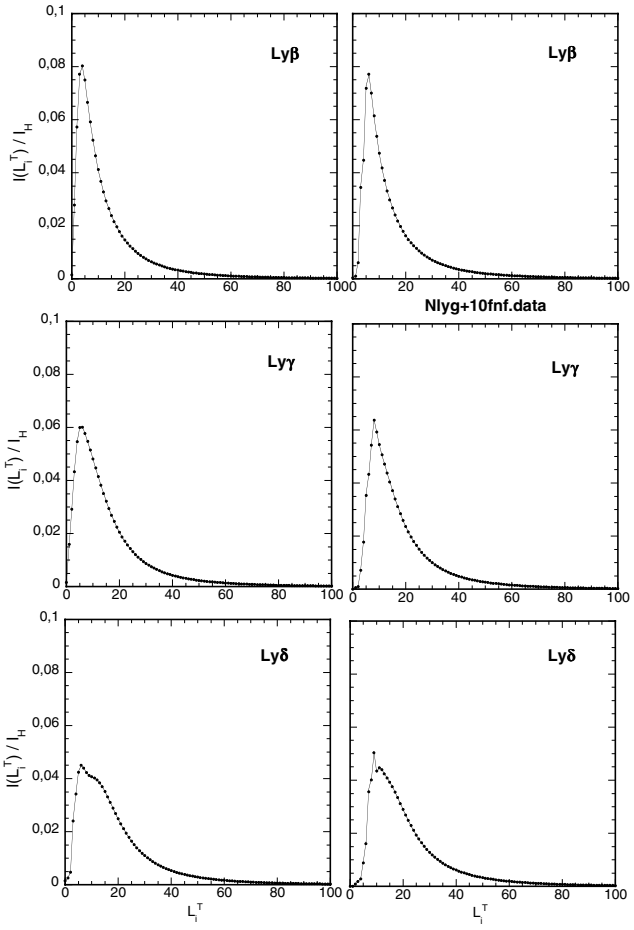

Fig. 2. Contribution at $T = 12\,200$ K of the first momenta L^T_i to the Lyβ, Lyγ, Lyδ lines at $\Delta\lambda = -10$ Å *(left)* and $\Delta\lambda = 10$ Å *(right)*. All the contributions are relative to the corresponding total Holtsmark intensities.

The same tendency is found for all the Lyman lines. Figure 2 presents the contributions of the first angular momenta for $\Delta\lambda = \pm 10$ Å and $T = 12\,200$ K (the values are relative to the corresponding Holtsmark intensity given for the three lines in Table 2).

3.3. Upper limit of L^T_i

The sum over L^T_i in Eq. (1) extends until $L^T_{Max} = L_D$, where $L_D = K\rho_D$ corresponds to a cutoff at the Debye radius $\rho_D = \sqrt{\frac{kT}{4\pi N_e e^2}}$ which gives $L_D = 4.02 \times 10^6 \frac{T}{\sqrt{N_e}}$. Values of L_D are given in Table 3 for $T = 12\,200$ K.

Table 2. Holtsmark profile (in frequency unit) for the Lyβ, Lyγ, Lyδ wings.

Lyβ	$I_{\rm H} = 48.266 \sqrt{\frac{\hbar}{m_{\rm e}}} (\Delta\omega)^{-\frac{5}{2}} N_{\rm e}$
Lyγ	$I_{\rm H} = 125.74 \sqrt{\frac{\hbar}{m_{\rm e}}} (\Delta\omega)^{-\frac{5}{2}} N_{\rm e}$
Lyδ	$I_{\rm H} = 265.05 \sqrt{\frac{\hbar}{m_{\rm e}}} (\Delta\omega)^{-\frac{5}{2}} N_{\rm e}$

Table 3. Values of the cut-off $L_{\rm D}^{\rm T}$ for several electronic densities $N_{\rm e}$, T = 12 200 K.

$N_{\rm e} \times {\rm cm}^{-3}$	$L_{\rm D}^{\rm T}$
10^{16}	573
10^{17}	155
10^{18}	49

From this table and Fig. 2, it appears that full convergence of the summation is not obtained at $N_{\rm e} = 10^{18}$ cm^{-3}, which leads to density effects in the profile intensity.

4. Results and discussion

All the calculations were performed with Mathematica: the accuracy of the results was tested for the Lyman α line by comparison with the Fortran code of Motapon (1998).

In Fig. 3, Holtsmark normalized profiles calculated for $N_{\rm e} = 10^{16}$ cm^{-3} are reported. At that density, convergence of the summation of the partial intensities is obtained before the Debye cutoff and no density effect occurs. We observe that the electronic profile in the wings gives a red wing higher than the blue wing. This asymmetry comes from the appropriate dynamical treatment with correct relation of conservation of energy, which gives a lower limit $\epsilon_{\rm min} = \hbar\Delta\omega$ of integration over the initial kinetic energy for $\Delta\omega > 0$. Such an effect cannot be found in a semi-classical treatment which assumes a constant relative velocity along the perturber trajectory and thus yields symmetric profiles (see tables by Vidal et al. 1973).

Figure 4 shows the variation of the profiles for different densities (T = 20 000 K). This variation due to the Debye cutoff is negligible in the wings due to the rapid convergence of the summation over $L_{\rm i}^{\rm T}$ in Eq. (1). As expected, some variations appear in the near wing at high densities.

As previously shown for the Lyman α line (Feautrier et al. 1976; Feautrier & Tran-Minh 1977; Tran-Minh et al. 1980), the Holtsmark profile underestimates the intensity in the near wing ($\Delta\lambda \leq 10$ Å) and overestimates the far wing. As explained above, the exact resonance method gives a lower limit of the contribution of the first angular momenta and as a consequence underestimates the intensity. As shown in Fig. 2, the relative contribution of the first angular momenta increases with decreasing temperatures leading to some uncertainties in the far wings at low temperatures (a few 1000 K). In that case, no approximate method is valid, and explicit account of short range and exchange interactions is needed. Such calculations using the R-Matrix method are in progress (Vo Ky Lan 2004).

The results obtained in the present work may be considered as correct in the near wing for all typical temperatures of star atmospheres and at higher temperatures (larger than 10 000 K) in the farther wings ($\Delta\lambda \leq 30$ Å). The results presented here as well as results for other temperatures and densities are available upon request from the authors.

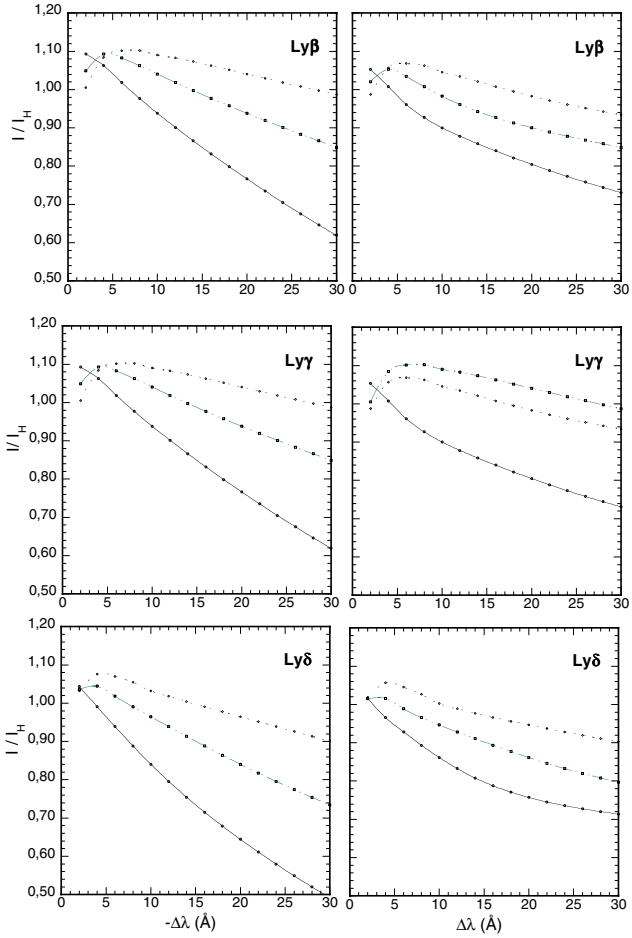

Fig. 3. Blue *(left)* and red *(right)* wing profiles of Lyβ, Lyγ, Lyδ lines for 3 electronic temperatures $T_{\rm e}$: full line: 5000 K, dashed-dotted line: 10 000 K, dotted line: 20 000 K

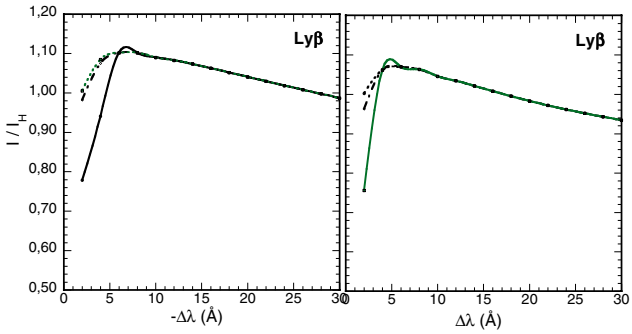

Fig. 4. Density effects on Lyβ blue wing *(left)* and red wing *(right)*. Dotted curve: $N_{\rm e} = 10^{16}$ cm^{-3}; dotted-plain curve: $N_{\rm e} = 10^{17}$ cm^{-3}; plain curve: $N_{\rm e} = 10^{18}$ cm^{-3}; T = 20 000 K.

Acknowledgements. A. Spielfiedel is gratefully acknowledged for helpful discussions and a careful reading of the manuscript The computations were performed on the work stations of the computer center of Observatoire de Paris.

Appendix A: μ_m values for the $n = 3$ level

Table A.1. Complex μ_m values for $n = 3$ (π_1=$(-1)^{l_i}$).

π_1	$L_i^T = 0$	$L_i^T = 1$	$L_i^T = 2$	$L_i^T = 3$	$L_i^T = 4$	$L_i^T = 5$
μ_1	4.02746	4.3524	4.9255	5.65777	6.48555	7.37063
μ_2	−0.5 + 3.99363i	−0.5 + 3.82718i	−0.5 + 3.46396i	4.51879	5.3668	6.26934
μ_3	2.83101	3.17009	3.76438	3.76438	4.21829	5.14494
μ_4	−0.5 − 2.51462i	1.91901	2.55171	2.80923	3.88452	4.92538
μ_5	1.54969	−0.5 + 2.2295i	1.64815	−0.5 + 2.81447i	2.51771	3.68226
μ_6	−0.5 + 1.4221i	0	−0.5 + 1.43161i	1.11578	−0.5 + 1.51995i	1.72213

Table A.2. Complex μ_m values for $n = 3$ (π_1=$(-1)^{l_i+1}$).

π_1	$L_i^T = 0$	$L_i^T = 1$	$L_i^T = 2$
μ_1	2.3101	3.17009	3.76438
μ_2	−0.5 + 2.51462i	−0.5 + 2.22925i	1.64815
μ_3	−0.5 + 1.4221i	0	−0.5 + 143161i

References

Baranger, M. 1958, Phys. Rev., 1129, 855

Feautrier, N., Tran-Minh N., & Van Regemorter, H. 1976, J. Phys. B: Atom. Molec. Phys., 9, 1871

Feautrier, N., & Tran-Minh, N. 1977, J. Phys. B: Atom. Molec. Phys., 10, 3427

Gradshteyn, I. S., & Ryzhik, I. M. 1965, Table of Series, Products and Integrals (New York: Academic Press)

de Kertanguy, A., Tran-Minh, N., & Feautrier, N. 1979, J. Phys. B: Atom. Molec. Phys., 12, 365

Motapon, O. 1998, A&A, 329, 792

Percival, I. C., & Seaton, M. J. 1957, Proc. Camb. Phil. Soc. 53, 654

Seaton, M. 1961, Proc. Phys. Soc., 77, 174

Tran-Minh, N., & Van Regemorter, H. 1972, J. Phys. B: Atom. Molec. Phys., 5, 903

Tran-Minh, N., Feautrier, N., & Van Regemorter, H. 1975, J. Phys. B: Atom. Molec. Phys., 8, 1810

Tran-Minh, N., Feautrier N., & Edmonds A. R. 1980, JQRST, 23, 377

Van Regemorter, H. 1969, Phys. Lett., 30A, 365

Vidal, C. R., Cooper, J., & Smith E. W. 1973, ApJS, 25, 37

Vo Ky Lan 2004, personal communication